A Unified Controller for Natural Ambulation on Stairs and Level Ground with a Powered Robotic Knee Prosthesis

Marissa Cowan,
Department of Mechanical Engineering and the Robotics Center at the University of Utah.

Suzi Creveling,
Department of Mechanical Engineering and the Robotics Center at the University of Utah.

Liam M. Sullivan,
Department of Mechanical Engineering and the Robotics Center at the University of Utah.

Lukas Gabert,
Department of Mechanical Engineering and the Robotics Center at the University of Utah.

Rocky Mountain Center for Occupational and Environmental Health.

Tommaso Lenzi
Department of Mechanical Engineering and the Robotics Center at the University of Utah.

Rocky Mountain Center for Occupational and Environmental Health.

Department of Biomedical Engineering at the University of Utah

Abstract

Powered lower-limb prostheses have the potential to improve amputee mobility by closely imitating the biomechanical function of the missing biological leg. To accomplish this goal, powered prostheses need controllers that can seamlessly adapt to the ambulation activity intended by the user. Most powered prosthesis control architectures address this issue by switching between specific controllers for each activity. This approach requires online classification of the intended ambulation activity. Unfortunately, any misclassification can cause the prosthesis to perform a different movement than the user expects, increasing the likelihood of falls and injuries. Therefore, classification approaches require near-perfect accuracy to be used safely in real life. In this paper, we propose a unified controller for powered knee prostheses which allows for walking, stair ascent, and stair descent without the need for explicit activity classification. Experiments with one individual with an above-knee amputation show that the proposed controller enables seamless transitions between activities. Moreover, transition between activities is possible while leading with either the sound-side or the prosthesis. A controller with these characteristics has the potential to improve amputee mobility.

Marissa corresponding author to provide marissa.cowan@utah.edu.

I. INTRODUCTION

Ambulation with conventional passive prostheses is generally slow, inefficient, and unstable [1]. Difficulty dealing with environmental barriers such as ramps, stairs, and uneven terrain often limits community ambulation [2]. Limited mobility negatively affects independence and quality of life [3] in individuals with lower limb amputations and can partly explain the high incidence of depression in this population [4]. Improved prosthesis technologies are necessary to meet the needs of individuals with above-knee amputations.

Powered lower-limb prostheses promise to improve mobility. Using embedded actuators, powered prostheses have the potential to replicate the biomechanical functions of the missing biological leg [5]–[8]. To accomplish this goal, powered prostheses need controllers that can coordinate the movements of the prosthetic joints with the user's residual and sound limbs, seamlessly adapting to the user's intended ambulation activity while dealing with the variability of the environment. Most powered prostheses aim to classify the user's intended ambulation activity (e.g., walking, stair climbing) in real-time, and then switch to a controller dedicated to that specific ambulation activity [9]–[12]. This approach has shown success in the laboratory, but translation to real-world use is an open question.

Activity classification is typically performed using machine learning. To train the machine learning algorithms, researchers have proposed using labelled data collected while amputee or nonamputee subjects ambulate in a laboratory environment which includes level-ground walking, stairs, and ramps [13]. The accuracy of the classification depends on the amount of data used for training [14], and can be improved using different kinds of sensors, including electromyography [13], sonomyography [15], range sensors [16], or cameras [17], in addition to prosthesis joint position and torque. Studies have shown higher than 95% offline classification accuracy. However, people take thousands of steps in a day, and any misclassification of the user's intended ambulation activity can cause the prosthesis to perform a different movement than the user expects [18], increasing the likelihood of falls and injuries. Therefore, nearly perfect accuracy is necessary for this "classify-and-switch" approach to succeed in real life.

In this paper, we show a unified controller for powered knee prostheses that seamlessly adapts to walking, stair ascent, and stair descent without explicit classification of the user's intended ambulation activity. The proposed controller continuously adapts the behavior of the powered prosthesis based on the movements of the user's residual thigh and the interaction of the prosthesis with the ground. Continuous adaptation is accomplished without making any assumptions about the user's intended activity (e.g., walk, climb stairs) or the characteristics of the environment (e.g., stair height). As a result, the proposed controller does not need to classify the intended ambulation activity or switch between activity-specific controllers. Different from previous studies, the proposed controller does not separate the movement into discrete, sequential phases [19], nor does it use a continuous phase evolution [20]. A controller with these characteristics may enable powered prostheses to support natural ambulation in the community, improving mobility for individuals with above-knee amputations. To assess the function of the proposed controller, one individual with an

above-knee amputation transitioned between walking, stair ascent, and stair descent using the proposed controller.

II. METHODS

A. Unified Controller

The proposed unified controller uses a simple finite-state machine (FSM) with two states, *Contact (C)* and *No Contact (NC),* as shown in Fig. 1(a). We use *Contact* and *No Contact* instead of *Stance* and *Swing* because we plan to extend this control architecture to activities which do not necessarily have *Stance* and *Swing* phases. When the axial ground reaction force (*GRF*) is greater than 60 N, the FSM switches to *Contact.* When the *GRF* is less than 20 N, the FSM switches to *No Contact.* Dedicated controllers are used in *Contact* and *No Contact* states. The transition between *Contact* and *No Contact* is defined as *Toe Off.* The transition between *No Contact* and *Contact* is defined as *Toe On.* The values of knee position, knee velocity, thigh position, and elapsed time, sampled at the transition between states, are used to continuously adapt the prosthesis behavior.

The *Contact* controller defines the desired knee torque (T_{Knee}) as the sum of three components as defined in (1).

$$T_{Knee} = T_{Step-Up} + T_{Biart} + T_{Damping}$$

(1)

The first component is the step-up torque ($T_{Step-Up}$), which follows a bell-shaped curve (Fig. 1(b)). The step-up torque mimics the biomechanical knee torque during stair ascent [21], [22] and sit-to-stand transitions [23] $T_{Step-Up}$ is adapted online similar to our stair ascent controller [21], [22]. The position at which the knee will reach maximum torque ($\theta_{Knee}^{T Max}$) is defined as a fixed percentage of the distance between the position of the knee at *Toe On* ($\theta_{Knee}^{Toe On}$) and the position of the knee at the end of the torque profile (θ_{Knee}^{End}), following (2). The maximum torque (T_{Knee}^{Max}) is proportional to $\theta_{Knee}^{Toe On}$, as shown in (3).

$$\theta_{Knee}^{T Max} = 0.8 \cdot (\theta_{Knee}^{Toe-On} - \theta_{Knee}^{End}) + \theta_{Knee}^{End}$$

(2)

$$T_{Knee}^{Max} = 1.2 \cdot \theta_{Knee}^{Toe On}$$

(3)

The second component defining the desired knee torque (T_{Knee}) is the biarticular torque (T_{Biart}). This component provides flexion torque which increases with the measured ankle torque (T_{Ankle}), following (4).

$$T_{Biart} = K_{Biart}^{Knee} \cdot K_{Biart}^{Thigh} \cdot T_{Ankle}$$

(4)

The gains K_{Biart}^{Knee} and K_{Biart}^{Thigh} change online based on the position of the knee (θ_{Knee}) and thigh (θ_{Thigh}) as shown in (Fig. 1(c–d)). K_{Biart}^{Thigh} forces T_{Biart} to zero when the user's residual thigh is in front of the user (i.e., negative thigh position). This action prevents the biarticular torque from causing the knee joint to buckle during level-ground walking or stair climbing. As the thigh moves from front to back, the value of K_{Biart}^{Thigh} increases from zero to one, enabling the powered knee to generate flexion torque as needed to initiate knee flexion in late stance during walking. Moreover, as the position of the knee increases, the value of K_{Biart}^{Knee} decreases to zero (Fig. 1(c)), preventing flexion torque from increasing indefinitely in late stance during walking.

The third component defining the desired knee torque is the damping torque ($T_{Damping}$), which is defined in (5).

$$T_{Damping} = -B \cdot \dot{\theta}_{knee}$$

(5)

The damping coefficient (B) switches based on the velocity of the knee ($\dot{\theta}_{Knee}$). If the knee is flexing ($\dot{\theta}_{Knee} > 0$ m/s), then the flexion damping is used ($B = B_{Flex}$). As shown in Fig. 1(e), B_{Flex} is a function of thigh position, and decreases from 0.15 Nms/deg to zero as the thigh moves from in front of the trunk ($\theta_{thigh} < 0°$) to behind it ($\theta_{thigh} > 0°$). While the knee is flexing, $T_{Damping}$ provides knee yielding (extension torque that slows the knee flexion) during level-ground walking and stair descent. When the knee is extending ($\dot{\theta}_{Knee} < 0°$), the extension damping is used ($B = B_{Ext}$). As shown in Fig. 1(f), B_{Ext} is a function of θ_{Knee}, and increases from zero to 0.1 Nm s/deg as the position of the knee decreases from 20° to 10°. In this condition, $T_{Damping}$ slows down the knee by providing positive flexion torque when the knee is close to full extension, reducing the impact when the knee joint reaches the mechanical end stop.

The No *Contact* controller defines the desired knee position ($\theta_{Knee}^{Desired}$) as the sum of two components, as shown in (6).

$$\theta_{Knee}^{Desired} = \theta_{MJ} + (K_{Syn} \cdot \theta_{Syn})$$

(6)

The first component is a minimum jerk trajectory (θ_{MJ}), calculated as in our previous work [19], [24], [25]. As shown in Fig. 1(g), given $\theta_{Knee}^{Toe\,Off}$ and a desired movement duration $Time_{des}[s]$, the proposed controller calculates a trajectory that minimizes the changes in acceleration. $Time_{des}$ is proportional to the duration of the previous *Contact* state.

The second component defining the desired knee position ($\theta_{Knee}^{Desired}$) is based on a synergistic movement of the thigh and knee (θ_{Syn}). This synergy is captured by a linear relationship between the thigh position and the knee position, as defined in (7) and shown in Fig. 1(h).

$$\theta_{Syn} = -1.1 \cdot \theta_{Knee}$$

(7)

θ_{Syn} is multiplied by an adaptive gain (K_{Syn}), which varies between zero and the sum of two terms as shown in (8).

$$K_{Syn} = K_{Syn}^0 + \Delta K_{Syn}$$

(8)

K_{Syn}^0 depends on $\theta_{Knee}^{Toe\,Off}$ (Fig. 1(i)). ΔK_{Syn} ensures that K_{Syn} is continuously adapted during the *No Contact* state. ΔK_{Syn} is initialized at zero every time the FSM transitions to *No Contact*. ΔK_{Syn} is then updated at every control iteration (n) using two algorithms to account for changes in the user's movement during the *No Contact* state. The first algorithm determines that when the user's thigh is in front of them, ΔK_{Syn} decreases as follows: If $-35° < \theta_{Thigh} < -10°$ and $\dot{\theta}_{Thigh} > -50\ m/s^2$, then $\Delta K_{Syn}(n+1) = \Delta K_{Syn}(n) - 0.008$. The second algorithm ensures that ΔK_{Syn} increases when the thigh is farther in front of the user as follows: If $\theta_{Thigh} < -35$ and $\dot{\theta}_{Thigh} < -20\ m/s^2$, then $\Delta K_{Syn}(\text{n}+1) = \Delta K_{Syn}(n) + 0.016$.

B. Powered Prosthesis

For this study, we used a modified version of the Utah Bionic Leg [8] combining the tah ionic Leg's powered knee module with a modified Ottobock Taleo ankle/foot prosthesis, as seen in Fig. 2(a). The powered knee module is a lightweight (1.6 kg), powered knee prosthesis that can actively generate torque and power during ambulation using a novel torque-sensitive actuator [26]. The Ottobock Taleo is a lightweight, carbon fiber ankle/foot prosthesis, capable of storing and returning energy during walking. For this study, we retrofit the Taleo with a custom GRF sensor made of titanium [27]. The titanium GRF sensor was connected to the carbon fiber using a custom aluminum part bolted to the carbon fiber. The weight of the device in the experimental configuration is 3.3 kg.

C. Experimental Protocol

We recruited one subject with a transfemoral (above-knee) amputation (30-year-old, male, 65 kg, 1.7 m, 9 years post-amputation). The subject had prior experience with the prosthesis and the proposed controller. Prior to the study, the subject provided written informed consent to participate, which included written consent to use photos and videos. All protocols for this study were approved by the University of Utah's Institutional Review Board.

After the powered prosthesis was properly aligned and fit, the subject familiarized himself with the powered prosthesis and the experimental protocol for about 15 minutes. The subject was able to comfortably walk and ascend/descend stairs using standard control parameters previously determined with pilot studies using a bypass adapter. However, we fine-tuned two

control parameters to better match his subjective preference. Specifically, we reduced B_{Flex} from 0.5 Nm s/deg to 0.15 Nm s/deg to decrease the knee resistance during stair descent and more closely match what the level of resistance that subject was used to with his prescribed prosthesis. Moreover, we increased the addendum in the equation that defines $\Delta K_{Syn}(n + 1)$ from 0.008 to 0.016 to allow for a faster knee extension when the subject starts walking from a standing position with the prosthesis-side first.

After familiarization, the subject rested for about 10 minutes. Then, data collection began. The experimental protocol required the subject to walk for two steps on level ground, climb a staircase with four steps, walk two steps on an elevated platform, turn around, walk two steps on the elevated platform, descend the same staircase, and walk two steps on level ground. First, the subject was asked to perform the sequence five times using his sound side to climb the first stair, referred to as "sound-side first". Next, the subject was asked to perform the sequence five times using his prosthesis to climb the first step, referred to as "prosthesis first" (Fig. 2(b)).

D. Data Acquisition and Processing

Data from the Utah Bionic Knee was saved at 500 Hz and processed offline using MATLAB. We filtered the raw data using a Butterworth filter with a cutoff of 8 Hz. We calculated joint velocities offline and filtered them with a 10 Hz Butterworth filter. We manually segmented the data into strides, defined from heel strike to heel strike on the prosthesis side. We analyzed the data in sequences of consecutive strides, each containing four strides: a walking stride, a transition stride, a stair ascent or stair descent stride, and a final walking or transition stride. The sequences are defined by the side used to climb the first step ("sound-side first" or "prosthesis first"), and whether the subject was ascending or descending the stairs ("walk-stair ascent-walk" or walk-stair descent-walk". Each sequence was repeated five times, and we selected the last three repetitions of each sequence for analysis in order to give the subject an opportunity to practice the walking sequence before actual data acquisition. For each sequence, we time-normalized and resampled each stride to 2,000 data points, and then calculated the time-average of the three repetitions.

III. RESULTS

The proposed unified controller enabled the subject to seamlessly transition between level-ground walking, stair ascent, and stair descent, leading either with their prosthesis or sound-side (Supplementary video). Visual inspection of the prosthesis kinematics and kinetics (Fig. 3) show substantial differences between the different sequences. These differences are discussed in the following subsections.

A. Walk – Stair Ascent – Walk

Focusing on the walk-stair ascent-walk sequence, we can see that the first stride for both prosthesis-side first (Fig. 3(a)) and sound-side first (Fig. 3(b)) is a purely walking stride. At *Toe On* (the transition between *No Contact* and *Contact*), the knee is fully extended ($\theta_{Knee} \sim 0°$). Therefore, the $T_{Step-Up}$ stays close to zero throughout *Contact*. As the user rolls over the prosthesis, the thigh moves from in front of the trunk ($\theta_{Thigh} < 0$) to behind the trunk

($\theta_{Thigh} > 0$) and the ankle/foot prosthesis is loaded in plantarflexion ($T_{Ankle} > 0$). As a result, T_{Biart} increases while $T_{Damping}$ goes to zero, causing the knee to flex in late stance. Due to the relatively high knee angle at *Toe Off* (the transition between *Contact* and *No Contact*) and the low absolute value of the thigh angle in swing, the synergy gain (K_{Syn}) stays close to zero for the whole duration of swing. However, a minimum-jerk trajectory is generated at *Toe Off*, which allows for adequate clearance during swing and drives the knee to full extension in preparation for the subsequent heel strike.

The second stride in the walk-stair ascent-walk sequences (Fig. 3(a–b)) is a transition stride between walking and stair ascent. This transition stride shows some meaningful differences between prosthesis first and sound-side first. When leading with the prosthesis side (Fig. 3(a)), the knee kinematics and kinetics during stance resemble those observed in the purely walking stride (described in the previous paragraph). In contrast, in swing, both the minimum-jerk (θ_{MJ}) and the synergy (θ_{Syn}) terms affect the knee kinematics. Specifically, as θ_{MJ} decreases and θ_{Syn} increases, keeping the knee flexed at a measured ~66° during *No Contact* to prepare for climbing the next step. When leading with the sound-side (Fig. 3(b)), the prosthetic knee joint remains fully extended during stance, with no biarticular, step-up or damping torque being generated. In swing, θ_{MJ} remains close to zero, while θ_{Syn} increases as the thigh angle decreases, driving the knee position to a measured 81° of flexion to prepare for climbing the next step.

The third stride in the walk-stair ascent-walk sequence (Fig. 3(a–b)) is a stair ascent stride. This third stride is quite similar when leading with the prosthesis and the sound-side. As the subject climbs the stair in *Contact*, the knee goes from flexed at ~56° to fully extended. $T_{Step-Up}$ is the main factor in driving the knee extension, peaking at ~−60 Nm, for both prosthesis and sound-side first. Moreover, as the knee gets closer to full extension, $T_{Damping}$ provides a positive flexion torque, peaking at ~28 Nm, which slows down the knee before it reaches full extension. In contrast, T_{Biart} stays close to zero for the whole stance duration. In swing, θ_{MJ} is close to zero and θ_{Syn} increases, driving the knee position to 85° of flexion to prepare for climbing the next step.

Finally, the fourth stride in the walk-stair ascent-walk sequence (Fig. 3(a–b)) is a transition stride between stair ascent and walking. For both prosthesis and sound-side first, stance resembles the non-transition stair ascent stance described in the previous paragraph (third stride). In contrast, swing differs substantially from previous strides. When leading with the prosthesis side, swing starts with θ_{Knee} close to zero. During swing, θ_{MJ} stays close to zero. In contrast, θ_{Syn} changes as the thigh moves, first generating knee flexion to clear the step, and then knee extension, as needed to prepare the prosthesis for the next step. When leading with the sound-side, swing resembles a purely walking stride, with the minimum-jerk defining the knee movement.

B. Walk – Stair Descent – Walk

The first and last stride in the walk-stair descent-walk sequences (Fig. 3(c–d)) are purely walking strides for both prosthesis and sound-side first. The knee position and torque for

these walking strides are virtually identical to the ones described for the first strides in the walk-stair ascent-walk sequences.

The second and third strides in the walk-stair descent-walk sequences are purely stair descent strides, regardless of the leading side. In stance, the leading knee is initially close to full extension ($\theta_{Knee} \sim 0$). As the subject loads the powered prosthesis, the knee starts flexing, peaking at ~82° at *Toe Off*. As the knee flexes, the flexion damping provides variable resistance to the movement, peaking at ~33 Nm. As the knee velocity at the end of stance is zero, the flexion damping torque is also zero. T_{Biart} and $T_{Step-Up}$ remain zero for the whole stance duration. In swing, θ_{Knee} starts at a relatively high flexion angle (~82 deg) and ends in an extended position. While θ_{MJ} goes to zero, θ_{Syn} initially increases, then decreases, causing the knee to extend slower than it would have without the contribution of θ_{Syn}.

IV. DISCUSSION

A. Significance

Powered prosthesis controllers need to quickly and seamlessly adapt to different ambulation activities in order to function in the real world. Most prosthesis controllers aim to address this issue by switching between activity-specific controllers based on the user's intended activity. However, this approach requires a perfect classification of the intended ambulation activity, which may not be achievable in the real world. In this paper, we propose a unified control approach based on continuous adaptation of the prosthesis to the movement of the user's residual limb and the interaction of the prosthesis with the ground. Our results show that the proposed unified controller can seamlessly adapt to walking on level ground, stair ascent, and stair descent without explicitly classifying the user's intended ambulation activity. Moreover, our experiments show that the proposed unified controller enables a subject to transition between these different ambulation activities while leading with either their prosthesis or their sound side. Thus, this study provides the first demonstration of a unified walking/stair controller for powered knee prostheses to the best of our knowledge.

Level-ground walking, stair ascent, and stair descent require different torques at the knee joint. During ground contact in the proposed unified controller, the desired torque is the sum of three components: $T_{Step-Up}$, $T_{Damping}$, and T_{Biart}. These three components are added together for all activities. However, they are not constant and change continuously based on the knee and thigh movements. As a result of this continuous adaptation, the $T_{Step-Up}$ primarily extends the knee during stair ascent but has little-to-no effect in stair descent and walking. $T_{Damping}$ produces the necessary knee yielding in stair descent but does not hamper knee flexion in walking. T_{Biart} initiates knee flexion during level-ground walking but does not do so during stair descent when extension torque is needed instead. Therefore, our results show that continuous adaptation provides the required torque for all these ambulation activities without knowing which one is being performed.

Ambulation on level-ground and on stairs requires a specific movement of the knee when the foot is in *No Contact*. The proposed unified controller generates swing movements by combining minimum-jerk programming (θ_{MJ}) and a bioinspired thigh-knee synergy (θ_{Syn}). A

minimum-jerk trajectory is generated every time the prosthetic foot is lifted from the ground and the endpoint of this trajectory is always zero—a fully-extended knee. However, due to the nature of minimum-jerk programming, the position trajectory stays close to zero when the knee angle at $Toe\ Off$ is close to zero, like in a purely stair ascent stride or when shuffling. In contrast, θ_{Syn} changes continuously based on the knee and thigh position. This desired knee trajectory due to θ_{Syn} is critical for stair ascent and has a substantial effect on stair descent. Interestingly, it does not affect a purely walking stride, but fully determines the knee movement in a stair-ascent-to-walking transition stride. Thus, our results show that the proposed controller enables modulation of the swing trajectory as necessary to accommodate variations both within- and between-ambulation activities while allowing for seamless transitions.

B. Limitations

There are some limitations to consider when interpreting the results of this study. The most important limitation is that only one subject was involved in the study. Therefore, we do not know if the proposed controller works for other amputee subjects. Moreover, we did not compare the prosthesis kinematics and kinetics with nonamputee datasets. Therefore, we do not know if the proposed controller restores normative gait. Adapting the controller parameters to the personal preferences of the subject in this study took less than five minutes, but it may take longer for other subjects. In some strides, there is a visible difference between the measured and the desired knee position. This result is due to the fact that we kept the gains of the position controller quite low (P=0.3 Nm/deg, I = 0; D=0.004 Nm s/deg) to leverage the passive dynamics of the knee prosthesis in order to maximize safety and efficiency. However, higher PID gains may produce better results. The testing environment was standardized. There is significantly more variability in the real-world and this controller needs to be tested in a non-standardized environment. Finally, we did not perform any stability analysis.

V. CONCLUSION

This study introduces the first unified controller for ambulation on level-ground and stairs with a powered knee prosthesis. Experiments with one individual with above-knee amputation show that the proposed unified controller allows for nearly seamless transitions between walking, stair ascent, and stair descent without using explicit classification. Because there is no classifier involved, there is no possibility of misclassification, which may lead to safer ambulation in the real world. Future work should focus on testing on a broader population as well as extending this unified controller to more activities.

Supplementary Material

Refer to Web version on PubMed Central for supplementary material.

Acknowledgments

REFERENCES

[1]. Schmalz T, Blumentritt S, and Jarasch R, "Energy expenditure and biomechanical characteristics of lower limb amputee gait:," Gait Posture, vol. 16, no. 3, 2002.

[2]. McGrath M et al. , "Can microprocessor knees reduce the disparity in trips and falls risks between above and below knee prosthesis users?," PLoS One, vol. 17, no. 9, p. e0271315, Sep. 2022. [PubMed: 36054087]

[3]. Pell JP, Donnan PT, Fowkes FGR, and Ruckley CV, "Quality of life following lower limb amputation for peripheral arterial disease," Eur J Vasc Surg, vol. 7, no. 4, 1993.

[4]. Wurdeman SR, Stevens PM, and Campbell JH, "Mobility Analysis of AmpuTees (MAAT I): Quality of life and satisfaction are strongly related to mobility for patients with a lower limb prosthesis," Prosthet Orthot Int, vol. 42, no. 5, 2018.

[5]. Lawson BE, Mitchell J, Truex D, Shultz A, Ledoux E, and Goldfarb M, "A robotic leg prosthesis: Design, control, and implementation," IEEE Robot Autom Mag, vol. 21, no. 4, 2014.

[6]. Azocar AF, Mooney LM, Duval JF, Simon AM, Hargrove LJ, and Rouse EJ, "Design and clinical implementation of an open-source bionic leg," Nat Biomed Eng, vol. 4, no. 10, 2020.

[7]. Elery T, Rezazadeh S, Nesler C, and Gregg RD, "Design and validation of a powered knee-ankle prosthesis with high-torque, low-impedance actuators," IEEE Transactions on Robotics, vol. 36, no. 6, 2020.

[8]. Tran M, Gabert L, Hood S, and Lenzi T, "A lightweight robotic leg prosthesis replicating the biomechanics of the knee, ankle, and toe joint," Sci Robot, vol. 7, no. 72, Nov. 2022.

[9]. Cheng S, Bolivar-Nieto E, Welker CG, and Gregg RD, "Modeling the Transitional Kinematics Between Variable-Incline Walking and Stair Climbing," IEEE Trans Med Robot Bionics, vol. 4, no. 3, pp. 840–851, Aug. 2022. [PubMed: 35991942]

[10]. Simon AM et al. , "Configuring a powered knee and ankle prosthesis for transfemoral amputees within five specific ambulation modes," PLoS One, vol. 9, no. 6, 2014.

[11]. Rezazadeh S, Quintero D, Divekar N, Reznick E, Gray L, and Gregg RD, "A phase variable approach for improved rhythmic and non-rhythmic control of a powered knee-ankle prosthesis," IEEE Access, vol. 7, 2019.

[12]. Varol HA, Sup F, and Goldfarb M, "Multiclass Real-Time Intent Recognition of a Powered Lower Limb Prosthesis," IEEE Trans Biomed Eng, vol. 57, no. 3, pp. 542–551, Mar. 2010. [PubMed: 19846361]

[13]. Hargrove LJ, Young AJ, and Simon AM, "Intuitive Control of a Powered Prosthetic Leg During Ambulation: A Randomized Clinical Trial," J Vasc Surg, vol. 63, no. 5, pp. 1405–1406, May 2016.

[14]. Young AJ and Hargrove LJ, "A Classification Method for User-Independent Intent Recognition for Transfemoral Amputees Using Powered Lower Limb Prostheses," IEEE Transactions on Neural Systems and Rehabilitation Engineering, vol. 24, no. 2, 2016.

[15]. Murray R, Mendez J, Gabert L, Fey NP, Liu H, and Lenzi T, "Ambulation Mode Classification of Individuals with Transfemoral Amputation through A-Mode Sonomyography and Convolutional Neural Networks," Sensors, vol. 22, no. 23, p. 9350, Dec. 2022. [PubMed: 36502055]

[16]. Liu M, Wang D, and Huang H, "Development of an Environment-Aware Locomotion Mode Recognition System for Powered Lower Limb Prostheses," IEEE Transactions on Neural Systems and Rehabilitation Engineering, vol. 24, no. 4, pp. 434–443, Apr. 2016. [PubMed: 25879962]

[17]. Krausz NE and Hargrove LJ, "Sensor Fusion of Vision, Kinetics, and Kinematics for Forward Prediction During Walking With a Transfemoral Prosthesis," IEEE Trans Med Robot Bionics, vol. 3, no. 3, pp. 813–824, Aug. 2021.

[18]. Zhang F, Liu M, and Huang H, "Effects of locomotion mode recognition errors on volitional control of powered above-knee prostheses," IEEE Transactions on Neural Systems and Rehabilitation Engineering, vol. 23, no. 1, 2015.

[19]. Lenzi T, Hargrove L, and Sensinger J, "Speed-adaptation mechanism: Robotic prostheses can actively regulate joint torque," IEEE Robot Autom Mag, vol. 21, no. 4, 2014.

[20]. Best TK, Welker CG, Rouse EJ, and Gregg RD, "Data-Driven Variable Impedance Control of a Powered Knee-Ankle Prosthesis for Adaptive Speed and Incline Walking," IEEE Transactions on Robotics, vol. 39, no. 3, pp. 2151–2169, Jun. 2023. [PubMed: 37304232]

[21]. Hood S, Creveling S, Gabert L, Tran M, and Lenzi T, "Powered knee and ankle prostheses enable natural ambulation on level ground and stairs for individuals with bilateral above-knee amputation: a case study," Sci Rep, vol. 12, no. 1, p. 15465, Sep. 2022. [PubMed: 36104371]

[22]. Hood S, Gabert L, and Lenzi T, "Powered Knee and Ankle Prosthesis With Adaptive Control Enables Climbing Stairs With Different Stair Heights, Cadences, and Gait Patterns," IEEE Transactions on Robotics, vol. 38, no. 3, pp. 1430–1441, Jun. 2022. [PubMed: 35686286]

[23]. Hunt GR, Hood S, Gabert L, and Lenzi T, "Effect of Increasing Assistance From a Powered Prosthesis on Weight-Bearing Symmetry, Effort, and Speed During Stand-Up in Individuals With Above-Knee Amputation," IEEE Transactions on Neural Systems and Rehabilitation Engineering, vol. 31, pp. 11–21, 2023. [PubMed: 36240032]

[24]. Tran M, Gabert L, Cempini M, and Lenzi T, "A Lightweight, Efficient Fully Powered Knee Prosthesis With Actively Variable Transmission," IEEE Robot Autom Lett, vol. 4, no. 2, pp. 1186–1193, Apr. 2019.

[25]. Mendez J, Hood S, Gunnel A, and Lenzi T, "Powered knee and ankle prosthesis with indirect volitional swing control enables level-ground walking and crossing over obstacles," Sci Robot, vol. 5, no. 44, Jul. 2020.

[26]. Tran M, Gabert L, and Lenzi T, "Analysis and Validation of Sensitivity in Torque-Sensitive Actuators," Actuators, vol. 12, no. 2, p. 80, Feb. 2023. [PubMed: 37008252]

[27]. Gabert L and Lenzi T, "Instrumented Pyramid Adapter for Amputee Gait Analysis and Powered Prosthesis Control," IEEE Sens J, vol. 19, no. 18, 2019.
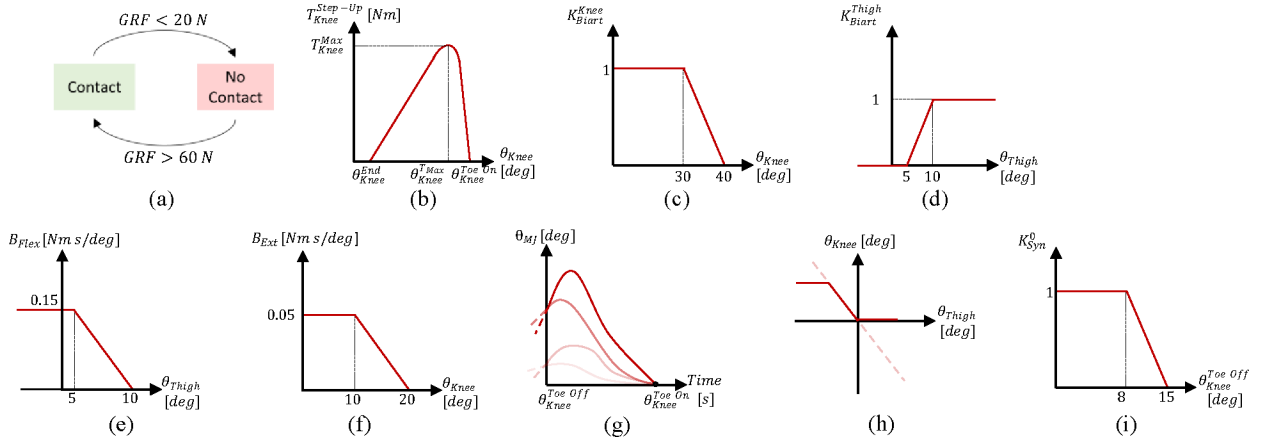
Fig. 1.

Controller Diagram. (a) State controller based on ground reaction force. (b) Step up torque as a function of knee position. (c) The biarticular gain of the knee as a function of the position of the knee at *Toe On*. (d) The biarticular gain of the thigh as a function of the position of the thigh at *Toe On*. (e) The flexion damping coefficient as a function of thigh position. (f) The extension damping coefficient as a function of knee position. (g) The minimum jerk trajectory with respect to time for multiple initial velocities and knee positions. (h) The relationship between knee position and thigh position. (i) The initial synergy gain as a function of knee position at *Toe Off*.
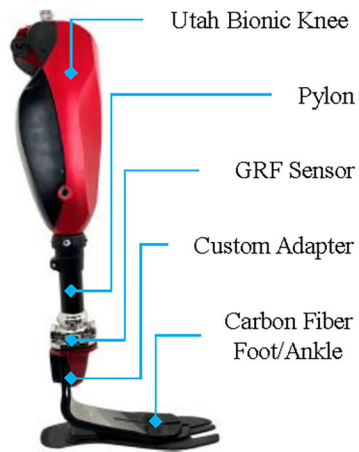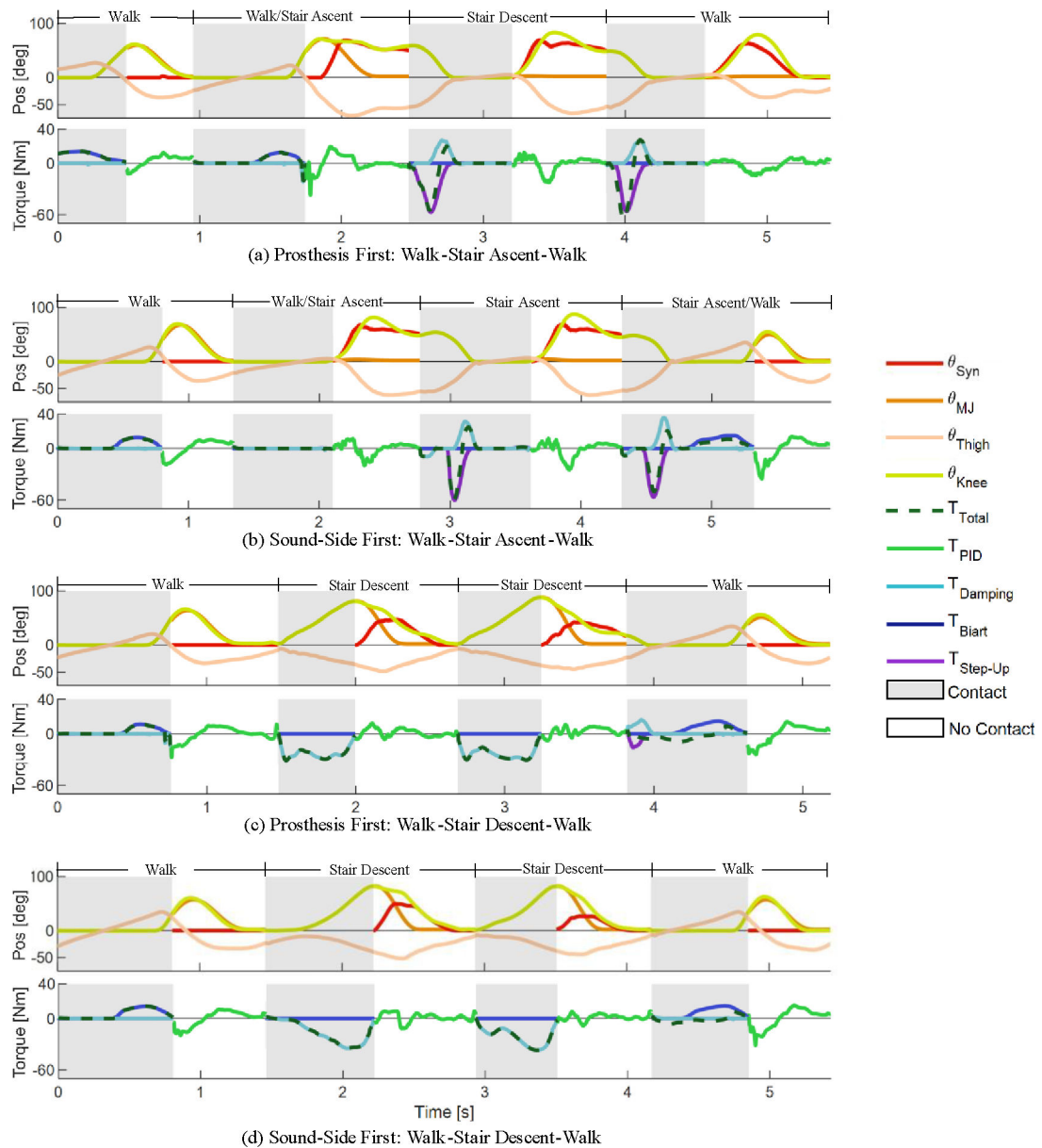
(a)   (b)

Fig. 2.
(a) The Utah Bionic Knee with the modified Taleo Ankle/Foot prosthesis. (b) A still-frame of the subject during prosthesis first stair ascent wearing the Utah Bionic Knee.

Fig. 3.
Experiment results. The top row of each subplot represents knee joint position data. The bottom row of each subplot represents knee joint torque data. Each stride contains a *Contact* (gray) and *No Contact* (white) section. (a) Prosthesis First: Walk-Stair Ascent-Walk. (b) Sound-Side First: Walk-Stair Ascent-Walk. (c) Prosthesis First: Walk-Stair Descent-Walk. (d) Sound-Side First: Walk-Stair Descent-Walk.